

The S-Wave Pion-Nucleon Scattering Lengths from Pionic Atoms using Effective Field Theory

S.R. Beane¹, V. Bernard², E. Epelbaum³,
Ulf-G. Meißner^{4,5} and D.R. Phillips⁶

¹*Department of Physics, University of Washington, Seattle, WA 98195, USA
E-mail: sbeane@phys.washington.edu*

²*Laboratoire de Physique Théorique
Université Louis Pasteur, F-67084 Strasbourg, France
E-mail: bernard@lpt6.u-strasbg.fr*

³*Ruhr-Universität Bochum, Institut für Theoretische Physik II,
D-44870 Bochum, Germany
E-mail: evgeni.epelbaum@tp2.ruhr-uni-bochum.de*

⁴*Forschungszentrum Jülich, Institut für Kernphysik (Th), D-52425 Jülich, Germany
E-mail: u.meissner@fz-juelich.de*

⁵*Karl-Franzens-Universität Graz, Institut für Theoretische Physik, A-8010 Graz, Austria*

⁶*Department of Physics and Astronomy, Ohio University, Athens, OH 45701, USA
E-mail: phillips@phy.ohiou.edu*

Abstract

The pion-deuteron scattering length is computed to next-to-next-to-leading order in baryon chiral perturbation theory. A modified power-counting is then formulated which properly accounts for infrared enhancements engendered by the large size of the deuteron, as compared to the pion Compton wavelength. We use the precise experimental value of the real part of the pion-deuteron scattering length determined from the decay of pionic deuterium, together with constraints on pion-nucleon scattering lengths from the decay of pionic hydrogen, to extract the isovector and isoscalar S-wave pion-nucleon scattering lengths, a^- and a^+ , respectively. We find $a^- = [0.0918(\pm 0.0013)] M_\pi^{-1}$ and $a^+ = [-0.0034(\pm 0.0007)] M_\pi^{-1}$.

PACS nos.: 13.75.Gx , 12.39.Fe

1 Introduction

The pion-nucleon (π -N) scattering lengths are quantities of fundamental importance in hadronic physics. They provide an important test of QCD symmetries and the pattern of their breaking. They also provide a crucial constraint on the π -N interaction and, as such, have an impact on our understanding of nucleon-nucleon (NN) scattering, the three-nucleon force, and pion-nucleus scattering.

In the limit of exact isospin symmetry the threshold π -N amplitude may be written as

$$T_{\pi N}^{ba} = 4\pi(1 + \mu) \left[\delta^{ba} a^+ + i\epsilon^{bac} \tau^c a^- \right] , \quad (1)$$

where $\mu \equiv M_\pi/m \simeq 1/7$ is the genuine small threshold parameter, and a^+ and a^- are the isoscalar and isovector S-wave scattering lengths, respectively. While these quantities cannot be measured directly in π -N scattering experiments, the well-known effective field theory (EFT), baryon chiral perturbation theory (χ PT), offers an ideal tool for extrapolating the π -N amplitude to threshold. Working up to fourth order in the dual momentum and pion-mass expansion, the values shown in Table 1 have been obtained from various analyses of π -N data [1, 2, 3, 4]. (Note that there are no fourth-order corrections to a^- [5]. The difference between the $O(p^3)$ and $O(p^4)$ values in Table 1 arises from a refitting of low-energy constants at lower orders, as discussed in Ref. [3].)

		$O(p)$	$O(p^2)$	$O(p^3)$	$O(p^4)$
a^+	Fit 1	0.0	0.0046	-0.0100	-0.0096
	Fit 2	0.0	0.0024	0.0049	0.0045
	Fit 3	0.0	0.0101	0.0014	0.0027
a^-	Fit 1	0.0790	0.0790	0.0905	0.0903
	Fit 2	0.0790	0.0790	0.0772	0.0771
	Fit 3	0.0790	0.0790	0.0870	0.0867

Table 1: Convergence of the S-wave scattering lengths for χ PT fits to the Karlsruhe [6], Matsinos [7], and VPI [8] phase-shift analyses of π -N data. $O(p^n)$ means that all terms up-to-and-including order n were included in the χ PT fit. Units are M_π^{-1} . Table taken from Ref. [3].

An independent approach to the π -N scattering lengths involves analyzing pionic-atom level shifts and widths. In the Coulombic π^- -p system, the strong-interaction shift in the energy can be used to infer a value for a^- . The recent Neuchatel-PSI-ETHZ (NPE) experiment [9] finds:

$$a^- = [0.0905(\pm 0.0042)] M_\pi^{-1} . \quad (2)$$

Note that the error here is significantly smaller than the spread of values obtained from the analyses of π -N scattering (see Table 1). Only the lifetime (or, equivalently, the width) of pionic hydrogen is sensitive to a^+ . The NPE experiment [9] finds the value:

$$a^+ = [-0.0022(\pm 0.0043)]M_\pi^{-1} . \quad (3)$$

Thus, neither π -N scattering nor the π^- -p atom provide a strong constraint on a^+ . The isoscalar scattering length may well be probed more directly in the π^- -deuterium atom. The NPE measurement [10] of the pionic-deuterium atomic-level shift yields:

$$a_{\pi d} = [-0.0261(\pm 0.0005) + i 0.0063(\pm 0.0007)]M_\pi^{-1} \quad (4)$$

for the pion-deuteron (π -d) scattering length—a measurement that is remarkably accurate given the usual level of precision in hadronic-physics experiments ¹. In order to precisely relate this number to a^+ an EFT of threshold π -d scattering is required.

There has been remarkable recent progress in developing the EFTs relevant to multi-nucleon systems [12, 13]. Among the advantages of this formalism is a quantitative method for estimating theoretical errors and a unified field-theoretic treatment of processes involving different numbers of nucleons. The non-perturbative effects responsible for deuteron binding are accounted for in the EFT power-counting, with a meaningful quantification of the theoretical error. The multi-nucleon EFT relevant to momentum transfers of order the pion mass is in most cases a straightforward generalization of single-nucleon baryon χ PT [14, 15, 16]. NN phase shifts and deuteron properties have now been computed to next-to-next-to-leading order (NNLO= $O(p^3)$) for the NN potential, where p (p denotes a small momentum/pion mass) in this expansion [17, 18, 19]. Processes with external pions and photons have also been extensively studied [13].

Consider π -d scattering at threshold [20, 21]. Two-pion-four-nucleon operators which contribute to π -d scattering enter at high orders in the EFT expansion and are therefore highly suppressed [20]. That these contributions are very small is crucial to the predictive power of the EFT, as the coefficients which determine the strength of these operators are unknown, and need therefore be determined from a separate nuclear observable, or, at some time in the distant futurity, from lattice QCD [16]. This suppression of local operators has an associated benefit: the π -d scattering length is sensitive to low-energy constants which contribute to the S-wave π -N scattering lengths, a^- and a^+ .

While baryon χ PT provides a rigorous theory of low-energy π -d scattering, there is an important kinematical subtlety in the threshold region; this leads to a new EFT [22] which distinguishes between the low scales M_π and γ , where γ is the deuteron binding momentum. This straightforward generalization of baryon χ PT turns out to be an extremely useful tool in developing a precise theoretical relation between the π -d and π -N S-wave scattering lengths.

¹For a general introduction to the π -d scattering length and its significance see Ref. [11].

Some additional remarks are in order. First, we should mention that the EFTs used in this paper can be applied to scattering and bound-state observables. For the direct extraction of the S-wave scattering lengths from pionic atoms one can also use the bound-state EFT as applied, for example, to π^- -p atoms in Ref. [23]. Since that approach is designed to deal with the pionic-hydrogen system, it is expected to give better control of the theoretical errors. However, for the case of pionic deuterium one faces a genuine three-body problem, which so far has not been formulated in the bound-state EFT, whereas it is straightforward to deal with in our approach. Second, throughout this work, we neglect isospin violation. Isospin violation has been worked out in the π -N system to $O(p^3)$ [24] and in NN scattering to NLO [25, 26, 27] but it goes beyond the scope of the present paper to systematically include it in the three-body system.

In Section 2 we extend the baryon χ PT analysis of the π -d scattering length to next-to-next-to leading order ($O(p^4)$). We then formulate a modified power-counting in Section 3 with which we derive an expression to extract the S-wave π -N scattering lengths from pionic-atom data. A comparison with other extractions of these quantities from the pionic-atom data is presented in Section 4. We conclude in Section 5.

2 The π -d Scattering Length in Baryon χ PT

We decompose the π -d scattering length as [20, 21]

$$a_{\pi d} = \frac{(1 + \mu)}{(1 + \mu/2)}(a_{\pi n} + a_{\pi p}) + a_{(boost)} + a_{(3-body)} + i \text{Im } a_{\pi d}. \quad (5)$$

Each of the various contributions on the right-hand side of Eq. (5) will be discussed in turn.

2.1 The isoscalar scattering length contribution

We first consider the “two-body” contributions where the pion interacts with a single nucleon, while the other nucleon acts as a spectator. This contribution to $a_{\pi d}$ is proportional to the isoscalar S-wave π -N scattering length,

$$a_{\pi n} + a_{\pi p} = 2a^+. \quad (6)$$

This quantity has been computed to $O(p^3)$ [28] and $O(p^4)$ [3] in baryon χ PT. Characteristic diagrams are shown in Fig. 1. The next-to-leading order (NLO= $O(p^3)$ for the amplitude) result is [28]

$$4\pi(1 + \mu)a^+ = \frac{M_\pi^2}{F_\pi^2} \left(\Delta - \frac{g_A^2}{4m} \right) + \frac{3g_A^2 M_\pi^3}{64\pi F_\pi^4}, \quad (7)$$

where $\Delta \equiv -4c_1 + 2c_2 + 2c_3$ and the c_i are low-energy constants. At this order there is a rather large spread in the values of a^+ resulting from fitting the low-energy constants to pion-nucleon phase-shift analyses [1, 2, 3, 4] (see Table 1). As pointed out above, measurement of the width of pionic hydrogen does not ameliorate this problem significantly, since the resulting value of a^+ is consistent with zero, and the error bar is too large to facilitate an accurate extraction of Δ .

The pionic-hydrogen measurement does constrain a^- quite strongly. On the theoretical front, we have the $O(p^4)$ expression for the isovector S-wave π -N scattering length [5, 29]:

$$4\pi(1 + \mu)a^- = \frac{M_\pi}{2F_\pi^2} + \frac{4M_\pi^3}{F_\pi^2} \left(\bar{D} + \frac{g_A^2}{32m^2} \right) + \frac{M_\pi^3}{16\pi^2 F_\pi^4} \quad (8)$$

where $\bar{D} \equiv \bar{d}_1 + \bar{d}_2 + \bar{d}_3 + 2\bar{d}_5$ and the \bar{d}_i are low-energy constants that have been fit to π -N phase shifts in Refs. [1] and [2]. The NPE pionic-hydrogen measurement gives the value quoted in Eq. (2), which allows for a determination of the combination of constants \bar{D} .

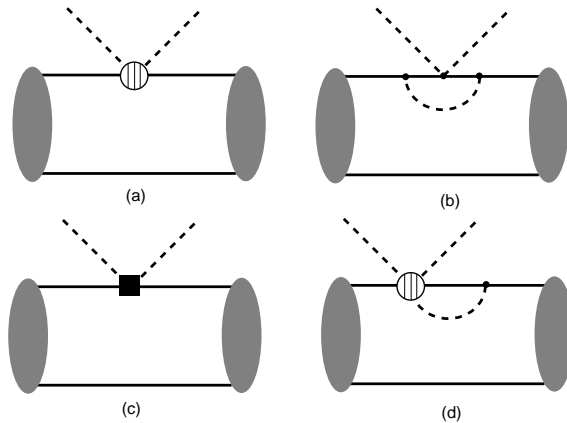


Figure 1: Characteristic two-body Feynman graphs which contribute to the π -d scattering length at $O(p^2)$ (a), $O(p^3)$ (b) and $O(p^4)$ (c),(d). The dots are leading-order vertices from $\mathcal{L}_{\pi N}^{(1)}$, the shaded blobs are from $\mathcal{L}_{\pi N}^{(2,3)}$, and the solid square is from $\mathcal{L}_{\pi N}^{(4)}$.

2.2 The boost correction

We now turn to the other contributions to $a_{\pi d}$ that can be reliably computed in baryon χ PT. The piece “ $a_{(boost)}$ ” (sometimes known as the “Fermi motion” correction) is a contribution to $a_{\pi d}$ from the graph Fig. 1(a), where the sliced blob represents a momentum-dependent vertex from the $O(p^2)$ chiral Lagrangian, $\mathcal{L}_{\pi N}^{(2)}$. This vertex would vanish if the

π -N system were at rest, but it contributes to π -d scattering, since the π -N amplitude must be boosted from the π -N center-of-mass frame to the π -d center-of-mass frame. This boost produces an $O(p^4)$ effect:

$$a_{(boost)} = -\frac{1}{2\pi(1 + \mu/2)} \frac{M_\pi^2}{4m^3 F_\pi^2} (g_A^2 - 8m c_2) \langle \vec{p}^2 \delta^{(3)}(\vec{q}) \rangle_{wf}, \quad (9)$$

where $\vec{q} \equiv \vec{p} - \vec{p}'$ and \vec{p} and \vec{p}' are, respectively, the initial and final-state relative momenta of the two nucleons, and

$$\langle \vartheta(\vec{q}) \rangle_{wf} \equiv \int d^3\vec{p} d^3\vec{p}' \Psi_d^\dagger(\vec{p}) \vartheta(\vec{q}) \Psi_d(\vec{p}'), \quad (10)$$

where Ψ_d is the deuteron wavefunction. The three-dimensional delta-function in Eq. (9) appears inside the expectation value since this boost effect is a “two-body” contribution to $a_{\pi d}$. Note that here the momentum-space deuteron wavefunctions are normalized so that:

$$\langle \delta^{(3)}(\vec{q}) \rangle_{wf} = 1. \quad (11)$$

2.3 Three-body effects

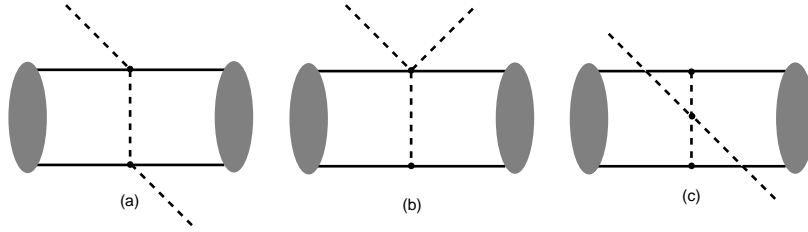


Figure 2: Three-body Feynman graphs which contribute to the π -d scattering length at $O(p^3)$ in baryon χ PT.

The dominant piece of the “three-body” amplitude, which occurs at $O(p^3)$ and is shown in Fig. 2, was written down some time ago by Weinberg [20],

$$a_{(3-body)}^{2a} = -\frac{M_\pi^2}{32\pi^4 F_\pi^4 (1 + \mu/2)} \left\langle \frac{1}{\vec{q}^2} \right\rangle_{wf}; \quad (12)$$

$$a_{(3-body)}^{2bc} = \frac{g_A^2 M_\pi^2}{128\pi^4 F_\pi^4 (1 + \mu/2)} \left\langle \frac{\vec{q} \cdot \vec{\sigma}_1 \vec{q} \cdot \vec{\sigma}_2}{(\vec{q}^2 + M_\pi^2)^2} \right\rangle_{wf}. \quad (13)$$

Nominal $O(p^4)$ corrections to these three-body effects are shown in Fig. 3. The new vertices appearing in these graphs are from $\mathcal{L}_{\pi N}^{(2)}$. Amusingly, these amplitudes cancel according to the following pattern:

$$\mathcal{M}_{(c)} = \mathcal{M}_{(d)} = \mathcal{M}_{(e)} = 0; \quad (14)$$

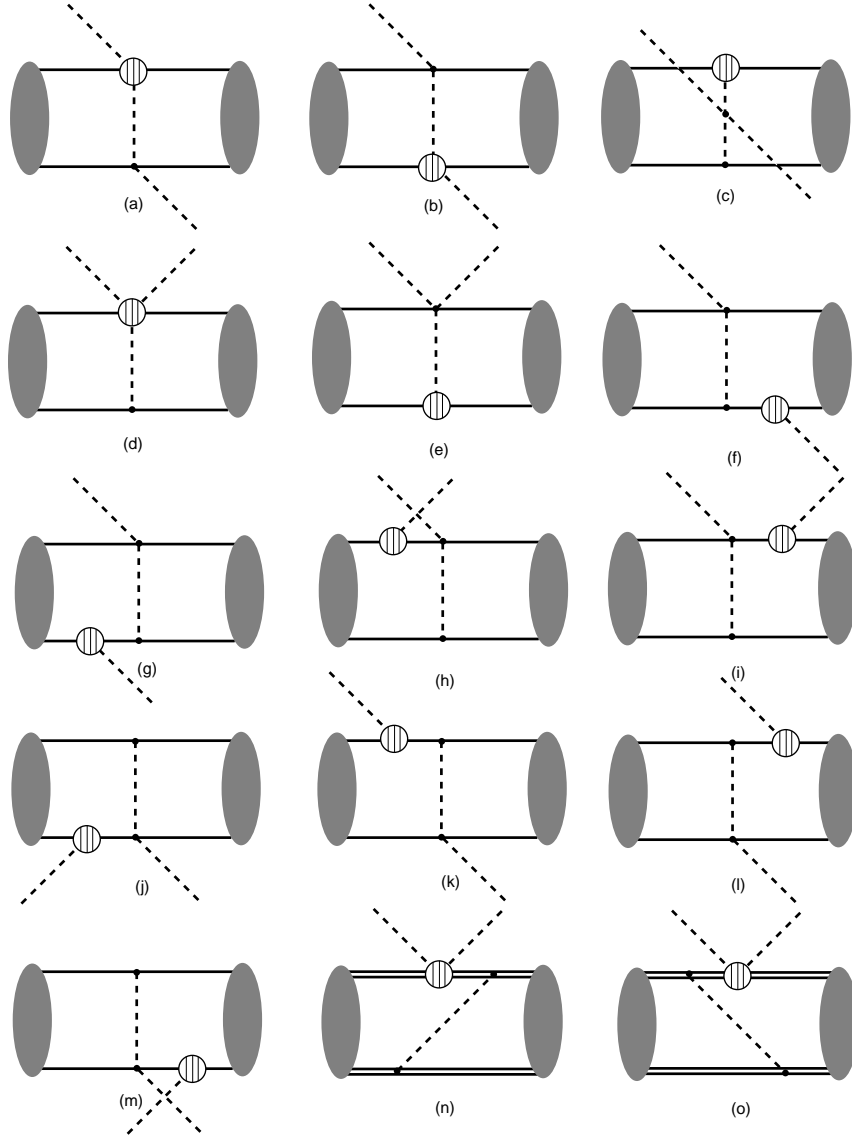


Figure 3: Three-body Feynman graphs which contribute to the π -d scattering length at $O(p^4)$ in baryon χ PT. The double lines indicate graphs evaluated in time-ordered perturbation theory.

$$\mathcal{M}_{(a)} + \mathcal{M}_{(b)} = 0; \quad (15)$$

$$\mathcal{M}_{(f)} + \mathcal{M}_{(g)} + \mathcal{M}_{(k)} + \mathcal{M}_{(l)} = 0; \quad (16)$$

$$\mathcal{M}_{(h)} + \mathcal{M}_{(j)} + \mathcal{M}_{(i)} + \mathcal{M}_{(m)} = 0; \quad (17)$$

$$\mathcal{M}_{(n)} + \mathcal{M}_{(o)} = 0. \quad (18)$$

Thus there is no three-body correction to $a_{\pi d}$ at order $O(p^4)$. The sum of all corrections vanishes for a variety of reasons, among them the threshold kinematics and the isoscalar character of the deuteron.

2.4 Results

This completes the computation of $a_{\pi d}$ to $O(p^4)$ in baryon χ PT². The pieces not proportional to a^+ are $a_{(3\text{-body})}$, which is simply the $O(p^3)$ expression given in Eqs. (12)–(13), and $a_{(boost)}$, which is obtained by taking an expectation value of the one-body operator p^2 between deuteron wavefunctions—see Eq. (9). The deuteron wavefunction computed with the NLO ($O(p^2)$) χ PT NN potential gives a consistent determination of $a_{\pi d}$ to $O(p^4)$. We have also shown results for the “NNLO*” χ PT NN potential which yields a node-less deuteron wavefunction, and the NNLO χ PT NN potential, whose deuteron wavefunction has two nodes. These nodes signal the presence of unphysical, deeply-bound states. The numerical results for the various contributions to $a_{\pi d}$ are shown in Table 2. The param-

	NLO		NNLO*		NNLO	
	500 MeV	600 MeV	500 MeV	600 MeV	900 MeV	1050 MeV
Λ [MeV]						
$a_{(boost)}$, Fit 1	0.00369	0.00511	0.00375	0.00419	0.03243	0.03379
$a_{(boost)}$, Fit 2	0.00350	0.00486	0.00357	0.00399	0.03084	0.03213
$a_{(boost)}$, Fit 3	0.00361	0.00501	0.00368	0.00411	0.03180	0.03313
$a_{(3\text{-body})}^{2a}$	−0.01954	−0.01864	−0.02057	−0.02056	−0.02360	−0.02257
$a_{(3\text{-body})}^{2bc}$	−0.00017	−0.00035	−0.00018	−0.00038	0.00033	0.00018
$\langle 1/\vec{q}^2 \rangle_{wf} [M_\pi]$	12.6	12.0	13.2	13.2	15.2	14.5
$\langle 1/ \vec{q} \rangle_{wf} [M_\pi^2]$	8.17	6.20	10.21	10.20	26.28	24.78

Table 2: Numerical results for the contributions to $a_{\pi d}$ given in Eqs. (9),(12) and (13) as well as other overlaps discussed in the text. All scattering lengths are in units of M_π^{-1} . Λ is the cutoff in the NN system.

²We relegate discussion of the imaginary part of $a_{\pi d}$ to Section 4.

ter set $F_\pi = 92.4$ MeV, $g_A = 1.2843$ (note that we adjust g_A from the Goldberger-Treiman relation), $M_\pi = M_{\pi^+} = 139.57$ MeV and $m = (m_n + m_p)/2 = 938.92$ MeV is used in all expressions. For each of the three different χ PT NN potentials we vary Λ , the cutoff in the NN system, in order to estimate our theoretical error. The three values (Fits 1-3) quoted for $a_{(\text{boost})}$ correspond to values of c_2 fit to various phase shift analyses of π -N scattering [2] (Fits 1-3 in Table 1). For comparison, in Table 3 we give numerical results for the same quantities computed using various “realistic” potential models.

	Nijm 93	Nijm I	Nijm II	CD Bonn 2000	AV 18
$a_{(\text{boost})}$, Fit 1	0.00594	0.00541	0.00623	0.00480	0.00609
$a_{(\text{boost})}$, Fit 2	0.00564	0.00515	0.00592	0.00456	0.00579
$a_{(\text{boost})}$, Fit 3	0.00582	0.00531	0.00611	0.00470	0.00597
$a_{(3\text{-body})}^{2a}$	-0.01984	-0.01993	-0.01954	-0.02020	-0.01961
$a_{(3\text{-body})}^{2bc}$	-0.00074	-0.00070	-0.00074	-0.00055	-0.00075
$\langle 1/\vec{q}^2 \rangle_{wf} [M_\pi]$	12.8	12.8	12.6	13.0	12.6
$\langle 1/ \vec{q} \rangle_{wf} [M_\pi^2]$	7.80	8.26	7.23	8.70	7.39

Table 3: Numerical results for the contributions to $a_{\pi d}$ given in Eqs. (9),(12) and (13) as well as other overlaps discussed in the text, for various potential models: Nijmegen [30]; CD-Bonn 2000 [31]; AV-18 [32]. All scattering lengths are in units of M_π^{-1} .

The following points are worth noting:

1. The nodes in the NNLO wavefunction cause the anomalous change in $a_{(\text{boost})}$ (by an order of magnitude) between the NLO and NNLO evaluations. This anomaly can be understood as follows. The boost correction to $a_{\pi d}$ is proportional to $\langle p^2 \rangle_{wf}$. While the sum of $\langle p^2 \rangle_{wf}/m$ and $\langle V \rangle_{wf}$ —the expectation value of the NN potential—is constrained to be 2.225 MeV, the NNLO potential is very deep because it supports unphysical NN states bound by over one GeV. It naively follows that $\langle p^2 \rangle_{wf}$ will be much larger for the NNLO wavefunction than for wavefunctions without unphysical, deeply-bound NN states. Of course if renormalization is done properly, this sensitivity to short-distance physics should be absent in observables up to subleading effects in the EFT. Given this technical issue, which is currently under investigation, in this paper we discard results obtained with the NNLO wavefunction.
2. When evaluated with the chiral NLO and NNLO* wavefunctions the smaller pieces of the $O(p^3)$ three-body contribution, $a_{(3\text{-body})}^{2bc}$, are rather different from the results

given in Table 1 of Ref. [21]. In contrast, the difference between the evaluations of Table 3 and those of Ref. [21] is small and arises from the different value of g_A used in that paper. The spread in $a_{(3\text{-body})}^{2bc}$ values in Tables 2 and 3 reflects the sensitivity of this contribution to the (unphysical) short-range behavior of the deuteron wavefunction.

3. Lastly, and most importantly, in all cases $a_{(3\text{-body})}^{2a}$ is much larger than any other contribution to $a_{\pi d}$ —including the contribution from a^+ . This suggests that the baryon χ PT scaling of operators is not properly accounting for the characteristic scales present in the deuteron wavefunction. We will return to this important point in the next section.

3 A Modified Power-Counting

As pointed out by Weinberg [20], Feynman graphs of the type shown in Fig. 2(a) are larger than their naive baryon χ PT scaling suggests because of infrared enhancements resulting from the anomalously small deuteron binding energy. For all of the NN wavefunctions considered in Table 2, $a_{(3\text{-body})}^{2a}$ is larger than $a_{(3\text{-body})}^{2bc}$ by two orders of magnitude. This is mainly because in low-energy π -d scattering pions carry energy and momentum that puts external pion legs, as well as internal pion legs in diagrams such as Fig. 2(a), on or near the pion mass-shell. The amplitude in Fig. 2(a) would be infrared divergent if the deuteron were a zero-energy bound state. As it is, this divergence is softened by the fact that the two nucleons in the deuteron are off their mass-shell. But the amount by which they are off their mass-shell is far less than the pion mass, and therefore if these effects are to be correctly accounted for in the EFT, we must find a way to incorporate the infrared enhancement into the theory.

The completely consistent way to do this is to construct an EFT where non-relativistic nucleons interact via contact operators, and pions near their mass-shell are included as massless excitations. Thus, in π -d scattering the nucleons are largely static and the successive scattering of a pion off the two nucleons generates a Coulomb-like interaction between them [22]. In order to have the incoming and outgoing nucleons as well as all the pions in a process near their respective mass-shells, there must be an equal number of pions entering and leaving each interaction vertex. Processes with interaction vertices that have a different number of pions entering than leaving are represented by local operators (on the scale of M_π) in this “EFT with heavy pions” ($H\pi$ EFT). $H\pi$ EFT is organized as an expansion in γ/M_π , since physics at the scale of the pion mass is “integrated out” and only appears implicitly in the theory via constants in the Lagrangian. Effects contributing explicitly to π -d scattering in this EFT are two-body π -N scattering and “three-body” effects in the multiple-scattering series for the πNN system [22]. Other

effects, such as $a_{(3\text{-body})}^{2bc}$, are non-dynamical and are represented by a local two-pion-four-nucleon operator. This operator appears at leading order in the expression for $a_{\pi d}$ and its coefficient is undetermined in H π EFT, since it is set by pion-scale physics. This counterterm fixes the scale dependence of a logarithm that is formally divergent in the infrared limit, $\gamma \rightarrow 0$.

Here we will employ an economical way of recovering the hierarchy of scales $\gamma \ll M_\pi$ that motivates the construction of the H π EFT. We will work in the pionful theory with a modified power counting that accounts for the infrared enhancement of graphs in the multiple-scattering series for the πNN system. In practice this means that we are able to fix the strength of the counterterm by matching the results of H π EFT developed in Ref. [22] to those of baryon χ PT derived above.

If we denote a generic momentum inside deuterium by \vec{q} , then the baryon χ PT power-counting is predicated upon $|\vec{q}| \sim M_\pi$. One might instead expect $|\vec{q}| \sim \sqrt{-B_d m} \equiv \gamma$, where B_d and γ are the deuteron binding energy and momentum, respectively. These two scalings would be compatible if the deuteron binding energy were of natural size. However, $B_d = -2.225$ MeV is unnaturally small on the scale of hadronic physics, as is $\gamma = 45.7025$ MeV. The true scaling is thus $|\vec{q}| \sim M_\pi/3$, and this additional $1/3$ suppression has a dramatic effect on the ordering of operators.

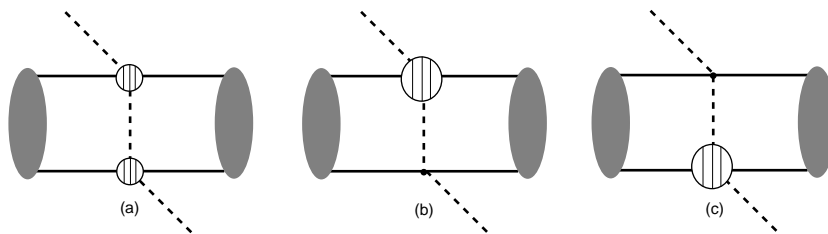


Figure 4: Infrared-enhanced Feynman graphs which contribute to the π -d scattering length at $O(p^5)$ in baryon χ PT and $O(Q^3)$ in the modified power-counting. The small shaded blobs are vertices taken from $\mathcal{L}_{\pi N}^{(2)}$ and the large shaded blobs are vertices taken from $\mathcal{L}_{\pi N}^{(3)}$ together with $O(p^3)$ one-loop graphs.

Hence we will adopt a modified scaling of operators in which $|\vec{q}| \sim p^2$ where p is the baryon χ PT expansion parameter³. Amplitudes involving M_π in the denominator are now suppressed, just as is the case in H π EFT. The expansion parameter for this modified power-counting is denoted by Q , where Q is the same size as p in baryon χ PT but, of course, leads to a different ordering of operators.

³Yet another power-counting for π -d scattering in which pions are purely perturbative has been studied in Ref. [33]. Unfortunately, it is now known that pions are strongly non-perturbative in the deuteron channel [34].

It is easy to check that in the modified power-counting $a_{(3\text{-body})}^{2a}$ is $O(Q)$ while $a_{(3\text{-body})}^{2bc}$ is $O(Q^5)$; thus, on the basis of scaling, $a_{(3\text{-body})}^{2bc}$ is expected to be much smaller than $a_{(3\text{-body})}^{2a}$. Meanwhile, the boost correction of Eq. (9) involves the expectation value inside the deuteron of two powers of momentum and a three-dimensional delta-function; and so scales as $O(Q^3)$.

In Table 4 we exhibit various contributions for a characteristic wavefunction and their scalings in both baryon χ PT and in the modified power-counting. The modified counting does a much better job of predicting the sizes of various mechanisms, presumably because it includes the full hierarchy of scales $\gamma \ll M_\pi \ll \Lambda_\chi$, where Λ_χ sets the breakdown scale of the chiral expansion.

	Baryon χ PT	Modified PC	NLO (500 MeV)	NLO (600 MeV)
$a_{(3\text{-body})}^{2a}$	$O(p^3)$	$O(Q^1)$	-0.01954	-0.01864
$a_{(\text{boost})}$ (Fit 1)	$O(p^4)$	$O(Q^3)$	0.00369	0.00511
$a_{(3\text{-body})}^5$	$O(p^5)$	$O(Q^4)$	0.00184	0.00175
$a_{(3\text{-body})}^{2bc}$	$O(p^3)$	$O(Q^5)$	-0.00017	-0.00035
$a_{(3\text{-body})}^{\text{range}}$, Ref. [35]	$O(p^5)$	$O(Q^5)$	0.00120	0.00041

Table 4: Scaling of various contributions to the scattering length in baryon χ PT and in the modified power-counting as discussed in the text. All matrix elements are evaluated with both the NLO (500 MeV) and the NLO (600 MeV) wavefunctions.

In the modified power-counting we do not yet have the full result at $O(Q^4)$. In particular, graphs of the type shown in Fig. 4 are promoted from their $O(p^5)$ scaling in baryon χ PT to $O(Q^3)$ in the modified counting. These graphs are corrections to $a_{(3\text{-body})}^{2a}$ with an insertion from $\mathcal{L}_{\pi N}^{(2)}$ at each vertex (Fig. 4(a)), or an insertion from $\mathcal{L}_{\pi N}^{(1)}$ at one vertex and $\mathcal{L}_{\pi N}^{(3)}$ at the other vertex (Fig. 4(b,c)). Computation of these graphs is straightforward. Fig. 4(a) evaluates to

$$a_{(3\text{-body})}^{4a} = \frac{M_\pi^4}{16\pi^4 F_\pi^4 (1 + \mu/2)} \left(\Delta - \frac{g_A^2}{4m} \right)^2 \left\langle \frac{1}{\vec{q}^2} \right\rangle_{\text{wf}}, \quad (19)$$

while Fig. 4(b) and Fig. 4(c) are given by

$$a_{(3\text{-body})}^{4bc} = -\frac{M_\pi^4}{8\pi^4 F_\pi^4 (1 + \mu/2)} \left[4 \left(\bar{D} + \frac{g_A^2}{32m^2} \right) + \frac{1}{16\pi^2 F_\pi^2} \right] \left\langle \frac{1}{\vec{q}^2} \right\rangle_{\text{wf}}. \quad (20)$$

The complete $O(Q^3)$ expression for the real part of the π -d scattering length is

$$\text{Re } a_{\pi d} = 2 \frac{(1 + \mu)}{(1 + \mu/2)} a^+ + a_{(\text{boost})} + a_{(3\text{-body})}^{2a} + a_{(3\text{-body})}^{4a} + a_{(3\text{-body})}^{4bc} \quad (21)$$

where the various terms can be found in Eqs. (7), (9), (12), (19) and (20), respectively. The astute reader will have noticed that to the order we are working we can rewrite Eq. (21) in the form

$$\text{Re } a_{\pi d} = 2 \frac{(1 + \mu)}{(1 + \mu/2)} \left(a^+ + (1 + \mu) [(a^+)^2 - 2(a^-)^2] \frac{1}{2\pi^2} \left\langle \frac{1}{\vec{q}^2} \right\rangle_{wf} \right) + a_{(boost)} + O(Q^4). \quad (22)$$

Thus, to $O(Q^3)$ the EFT with modified power-counting reproduces the simple intuitive picture of a single-scattering term plus a pion-exchange correction [11].

Notice that in the amplitudes of Fig. 4, the momentum dependence of the vertices from $\mathcal{L}_{\pi N}^{(2)}$ and $\mathcal{L}_{\pi N}^{(3)}$ has been neglected. While these corrections occur at the same order in baryon χ PT as Eq. (19) and Eq. (20) ($O(p^5)$), in the modified power-counting the momentum-dependent corrections begin at $O(Q^5)$ and are thus suppressed by two orders. These “range” corrections were recently computed in baryon χ PT [35]. The size of these contributions is consistent with the $O(Q^5)$ scaling (see Table 4). There are, of course, many other contributions at $O(Q^5)$, including two-pion-four-nucleon local operators with unknown coefficients⁴. As we will see below, there are many more important contributions at $O(Q^4)$ which are easily computed in the EFT. Hence we will not consider any $O(Q^5)$ effects in isolation, but will instead perform the complete calculation up to $O(Q^4)$ in the modified power-counting.

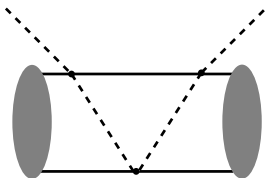


Figure 5: One-loop three-body diagram that contributes at $O(Q^4)$ in the modified power-counting and at $O(p^5)$ in baryon χ PT.

It is surprisingly easy to compute the $O(Q^4)$ corrections to the $O(Q^3)$ result, Eq. (22). There are no further two-body effects from the π -N amplitude at $O(Q^4)$. There are, of course, diagrams similar to those in Fig. 4 and Fig. 2(a), but with higher-order momentum-independent vertices. However, these corrections are already included in Eq. (22) since they are subsumed in a^\pm . There is then a single three-body one-loop graph, Fig. 5, representing the next term in the πNN multiple-scattering series. This contributes at $O(Q^4)$. Fig. 5 is one of many $O(p^5)$ baryon χ PT graphs that contribute to $a_{\pi d}$. However,

⁴It is, in a sense, unfortunate that these effects are suppressed, since one of the local operators at $O(Q^5)$ encodes information about the leading quark-mass dependence of the deuteron binding energy [16, 36].

the other graphs all have intermediate pions that are far from their mass-shell, and so are of higher order in the modified power-counting.

We have evaluated Fig. 5 using the leading-order χ PT π -N vertex for π -N scattering and have neglected contributions to the loop integral where pions are $\sim M_\pi$ off their mass-shell. These neglected contributions are again higher order in the modified power-counting. This gives:

$$a_{(3\text{-body})}^5 = \frac{1}{64\pi^4(1+\mu/2)} \left(\frac{M_\pi}{2F_\pi^2} \right)^3 \left\langle \frac{1}{|\vec{q}|} \right\rangle_{wf}. \quad (23)$$

Notice that, as in Eq. (12), this matrix element has a Coulomb-like propagator, which signals the presence of an infrared logarithm. It is this enhancement that is captured by the modified power-counting.

Our final formula for the π -d scattering length, valid to $O(Q^4)$ in the modified power-counting, is

$$\begin{aligned} \text{Re } a_{\pi d} = & 2 \frac{(1+\mu)}{(1+\mu/2)} \left(a^+ + (1+\mu) [(a^+)^2 - 2(a^-)^2] \frac{1}{2\pi^2} \left\langle \frac{1}{\vec{q}^2} \right\rangle_{wf} \right. \\ & \left. + (1+\mu)^2 [(a^+)^3 - 2(a^-)^2(a^+ - a^-)] \frac{1}{4\pi} \left\langle \frac{1}{|\vec{q}|} \right\rangle_{wf} \right) \\ & + a_{(boost)} + O(Q^5). \end{aligned} \quad (24)$$

where we have again subsumed higher-order effects into the π -N scattering lengths. Notice that since local two-pion-four-nucleon operators are not enhanced in the modified power-counting they appear at the same order as in baryon χ PT, namely fifth order, and do not affect the fourth-order result given in Eq. (24).

Equation (24) is easily inverted to give a constraint on a^+ and a^- in terms of the experimentally-determined $a_{\pi d}$ from Eq. (4). In order to evaluate the constraint we need the matrix elements $\langle 1/\vec{q}^2 \rangle_{wf}$ and $\langle 1/|\vec{q}| \rangle_{wf}$, as well as $a_{(boost)}$ (see Tables 2 and 3). The boost effect does depend on the chiral low-energy constant, c_2 , but this counterterm was fixed in Ref. [2] by fitting π -N phase shift data. The resulting relationship between a^- and a^+ is displayed in Fig. 6. Notice that we choose to plot a^+ vs $-a^-$, in order to facilitate comparison with other extractions.

The two bands in Fig. 6 correspond to two different evaluations of the deuteron matrix elements involved: one with the NLO wavefunction with an ultraviolet cutoff of 500 MeV (upper curve) and the other with a cutoff of 600 MeV (lower curve). In each case the finite width of the band arises from the error associated with the pionic-deuterium measurement of $a_{\pi d}$. The spread in the values of c_2 arising from Fits 1-3 of Table 1 also falls within these two bands. The result for a^+ found using ‘‘realistic’’ NN wavefunctions falls between these two bands, as, in most cases, would the effect of a typical $O(Q^5)$ correction. The experimental curves for the pionic-hydrogen shift and width are taken from Ref [9], while

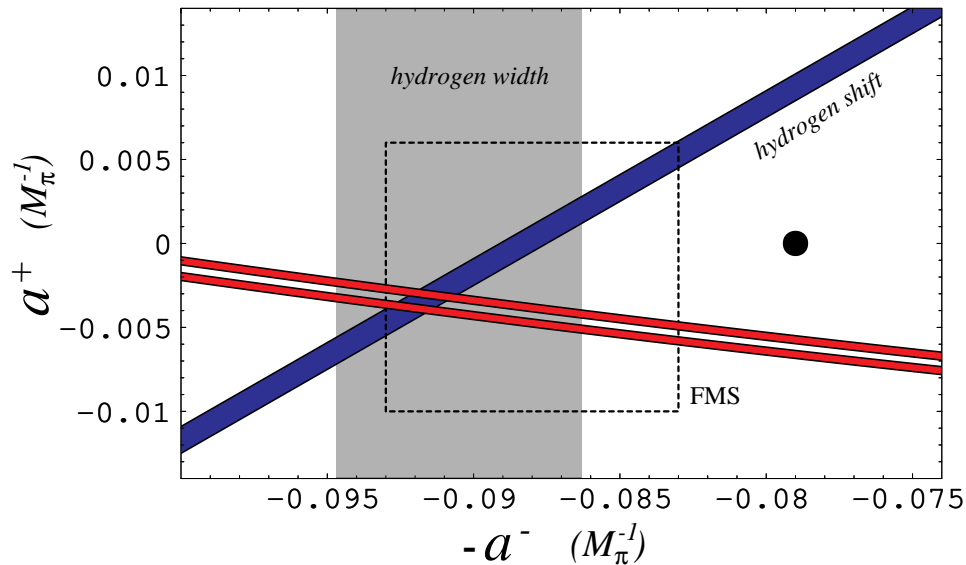


Figure 6: Plot of a^+ vs $-a^-$. The light shaded region and the dark band are from the experimental pionic-hydrogen width and shift, respectively, taken from Ref. [9]. The dotted line encompasses the constraints from π -N phase shift data and is taken from Ref. [2]. The dot is leading order χ PT (current algebra). The two parallel bands are from Eq. (24) evaluated with the NLO wavefunction with an ultraviolet cutoff of 500 MeV (upper curve) and 600 MeV (lower curve).

the bounds from baryon χ PT fits to π -N phase shift data are taken from Ref [2]. From the overlap region in this plot we extract the S-wave π -N scattering lengths. We find

$$\begin{aligned} a^- &= [0.0918(\pm 0.0013)] M_\pi^{-1}; \\ a^+ &= [-0.0034(\pm 0.0007)] M_\pi^{-1}. \end{aligned} \quad (25)$$

The theoretical error bars should be considered somewhat optimistic given our neglect of isospin violation.

4 Comparison with other extractions

The results of Eq. (25) are consistent with other recent extractions that do not make use of the EFT framework [37, 38]. In particular, they are in agreement with very recent work of Ericson and collaborators [38] who find $a^- = [0.0900(\pm 0.0016)] M_\pi^{-1}$ and $a^+ = [-0.0017(\pm 0.0010)] M_\pi^{-1}$. The calculation of Ref. [38] includes the basic mechanisms present in the EFT employed here, but also includes additional contributions to $a_{\pi d}$ which are higher order in the modified power-counting.

For instance, the analysis of Ref. [38] includes a “dispersive contribution” (with a sizeable error bar) that is numerically comparable to our $O(Q^3)$ boost correction (but with opposite sign). This contribution accounts for most of the numerical difference between the two analyses. However, we find that the “dispersive contribution” occurs only beyond the order to which we have worked in the modified power-counting.

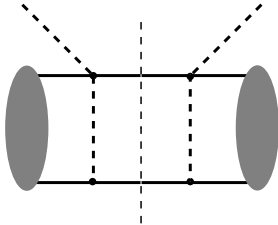


Figure 7: Characteristic one-loop three-body diagram that contributes at $O(p^5)$ in χ PT. This graph gives a contribution to the imaginary part of the π - d scattering length.

One graph which contributes to both the dispersive and absorptive parts of $a_{\pi d}$ is shown in Fig. 7. This three-body one-loop graph is one of the leading contributions to $\text{Im } a_{\pi d}$. It is $O(p^5)$ in baryon χ PT and $O(Q^6)$ in the modified power counting⁵. The $O(Q^6)$ scaling of Fig. 7 is seemingly at odds with the experimental value of $\text{Im } a_{\pi d}$ given in Eq. (4), which is consistent with an $O(Q^3)$ effect. It is easy to see why the scaling might break down for the imaginary part of the scattering length. The absorptive part of Fig. 7 is related by unitarity to the $\pi d \rightarrow NN$ process at threshold:

$$\text{Im } a_{\pi d} = \frac{1}{4\pi} \lim_{q \rightarrow 0} q \sigma(\pi^- d \rightarrow nn) \quad (26)$$

where q is the pion three-momentum in the π - d center-of-mass system. A study of $\pi d \rightarrow NN$ has been made in Ref. [39]. Unfortunately baryon χ PT applied to pion production significantly underpredicts the data. Presumably this is due to the large expansion parameter inherent in the pion-production process: since in this diagram momenta of order $\sqrt{mM_\pi}$ are present, the baryon χ PT expansion parameter is \sqrt{p} rather than p . Clearly this problem is present in any attempt to compute the absorptive contribution to the π - d scattering length in EFT, and is beyond the scope of this paper. Whether this is also an issue for the dispersive part is worth investigating, given the sizeable contribution claimed in Ref. [38]. We should also mention that Refs. [37] and [38] give an estimate of isospin violation that is consistent with an $O(Q^5)$ effect in the modified power counting. A systematic investigation of this very important issue within EFT is needed. Finally, our result for the isoscalar scattering length is consistent with a previous baryon χ PT determination at $O(p^3)$ [21]. Because a hybrid approach employing phenomenological wavefunctions was used in that paper, no theoretical error bar was given.

⁵Since pion number is not conserved at the interaction vertices, this graph appears as a two-pion-four-nucleon local operator in $H\pi$ EFT.

5 Conclusion

In this paper we have developed an EFT for the π -d scattering length. While naively, baryon χ PT, as modified by Weinberg [14] for the NN system, captures the correct hierarchy of scales, we have seen that there are several subtleties in the analysis of π -d scattering near threshold, which suggest a more practical power-counting. The new ingredient is the observation that one may develop a hierarchy between the pion mass, M_π and the deuteron binding momentum, γ . One can then pick out the pieces of the amplitude that become large in the formal limit in which γ goes to zero and M_π is held fixed [22]. This does not, of course, indicate that anything is amiss with baryon χ PT power-counting. Baryon χ PT should work just fine for π -d scattering in the threshold region, but high-order calculations are required if truly accurate results are desired. The advantage of the modified power-counting, and of EFT generally, is that it immediately isolates the large contributions, without requiring explicit calculations of matrix elements that end up being smaller than the theoretical error.

Acknowledgments:

We thank Martin Savage and Iraj Afnan for valuable conversations. DRP thanks Flinders University, where part of this work was performed, for its hospitality. This research was supported in part by the U. S. Department of Energy under grants DE-FG03-97ER41014 (SRB) and DE-FG02-93ER40756 (DRP), and by Deutsche Forschungsgemeinschaft under grant GL 87/34-1.

References

- [1] M. Mojžiš, Eur. Phys. J. **C2**, 181 (1998).
- [2] N. Fettes, Ulf-G. Meißner and S. Steininger, Nucl. Phys. **A640**, 199 (1998).
- [3] N. Fettes and Ulf-G. Meißner, Nucl. Phys. **A676**, 311 (2000).
- [4] P. Büttiker and Ulf-G. Meißner, Nucl. Phys. **A668**, 97 (2000).
- [5] V. Bernard, N. Kaiser and Ulf-G. Meißner, Phys. Rev. **C52**, 2185 (1995).
- [6] R. Koch, Nucl. Phys. **A448**, 707 (1986).
- [7] E. Matsinos, Phys. Rev. **C56**, 3014 (1997).
- [8] VPI/GW on-line phase-shift analysis, solution SP98. See URL <http://gwdac.phys.gwu.edu>.
- [9] H.C. Schröder *et al.*, Phys. Lett. **B469**, 25 (1999); Eur. Phys. J. **C21**, 473 (2001).
- [10] P. Hauser *et al.*, Phys. Rev. **C58**, 1869 (1998).
- [11] T. Ericson and W. Weise, “Pion and Nucleons” (Clarendon Press, Oxford, 1988).
- [12] E. Epelbaum *et al.*, *Prague 2001, Mesons and Light Nuclei*, AIP Conference Proceedings, Volume 603, Issue 1, (2001), nucl-th/0109065.
- [13] S.R. Beane, P.F. Bedaque, W.C. Haxton, D.R. Phillips and M.J. Savage, *At the Frontier of Particle Physics*, ed. M. Shifman, (World Scientific, 2001), nucl-th/0008064; P.F. Bedaque and U. van Kolck, nucl-th/0203055; D.R. Phillips, nucl-th/0203040.
- [14] S. Weinberg, Phys. Lett. **B251**, 288 (1990).
- [15] S. Weinberg, Nucl. Phys. **B363**, 3 (1991).
- [16] S.R. Beane, P.F. Bedaque, M.J. Savage and U. van Kolck, Nucl. Phys. **A700**, 377 (2002).
- [17] C. Ordoñez, L. Ray and U. van Kolck, Phys. Rev. **C53**, 2086 (1996).
- [18] E. Epelbaum, W. Glöckle and Ulf-G. Meißner, Nucl. Phys. **A637**, 107 (1998).
- [19] E. Epelbaum, W. Glöckle and Ulf-G. Meißner, Nucl. Phys. **A671**, 295 (2000).
- [20] S. Weinberg, Phys. Lett. **B295**, 114 (1992).
- [21] S.R. Beane, V. Bernard, T.S. Lee and Ulf-G. Meißner, Phys. Rev. **C57**, 424 (1998).

- [22] S.R. Beane and M.J. Savage, `nucl-th/0204046`.
- [23] V.E. Lyubovitskij and A. Rusetsky, *Phys. Lett.* **B494**, 9 (2000); J. Gasser *et al.*, `hep-ph/0206068`; *private communication*.
- [24] N. Fettes and Ulf-G. Meißner, *Nucl. Phys.* **A693**, 693 (2001).
- [25] U. van Kolck, *Few-Body Systems Suppl.* **9**, 444 (1995).
- [26] E. Epelbaum and Ulf-G. Meißner, *Phys. Lett.* **B461**, 287 (1999).
- [27] M. Walzl, Ulf-G. Meißner and E. Epelbaum, *Nucl. Phys.* **A693**, 663 (2001)
- [28] V. Bernard, N. Kaiser and Ulf-G. Meißner, *Nucl. Phys.* **A615**, 483 (1997).
- [29] V. Bernard, N. Kaiser and Ulf-G. Meißner, *Phys. Lett.* **B309**, 421 (1993).
- [30] V.G.J. Stoks et al., *Phys. Rev.* **C49** (1994) 2950.
- [31] R. Machleidt, *Phys. Rev.* **C63** (2001) 024001.
- [32] R.B. Wiringa et al., *Phys. Rev.* **C51** (1995) 38.
- [33] B. Borasoy and H.W. Griebhammer, `nucl-th/0105048`.
- [34] S. Fleming, T. Mehen and I.W. Stewart, *Nucl. Phys.* **A677**, 313 (2000).
- [35] N. Kaiser, *Phys. Rev.* **C65**, 057001 (2002).
- [36] S.R. Beane and M.J. Savage, `hep-ph/0206113`.
- [37] V.V. Baru and A.E. Kudryatsev, *Phys. Atom. Nucl.* **60**, 1475 (1997).
- [38] T.E. Ericson, B. Loiseau and A.W. Thomas, `hep-ph/0009312`.
- [39] C. da Rocha, G. Miller and U. van Kolck, *Phys. Rev.* **C61**, 034613 (2000).